

# Measurement of the Casimir force between dissimilar metals

R. S. Decca<sup>1</sup>, D. López<sup>2</sup>, E. Fischbach<sup>3</sup>, D. E. Krause<sup>4,3</sup>

<sup>1</sup>*Department of Physics, Indiana University- Purdue*

*University Indianapolis, Indianapolis, IN 46202, USA*

<sup>2</sup>*Bell Laboratories, Lucent Technologies, Murray Hill, NJ 07974, USA*

<sup>3</sup>*Department of Physics, Purdue University, West Lafayette, IN 47907, USA*

<sup>4</sup>*Physics Department, Wabash College, Crawfordsville, IN 47933, USA*

(Dated: October 26, 2018)

## Abstract

The first precise measurement of the Casimir force between dissimilar metals is reported. The attractive force, between a Cu layer evaporated on a microelectromechanical torsional oscillator, and an Au layer deposited on an Al<sub>2</sub>O<sub>3</sub> sphere, was measured dynamically with a noise level of 6 fN/ $\sqrt{\text{Hz}}$ . Measurements were performed for separations in the 0.2-2  $\mu\text{m}$  range. The results agree to better than 1% in the 0.2-0.5  $\mu\text{m}$  range with a theoretical model that takes into account the finite conductivity and roughness of the two metals. The observed discrepancies, which are much larger than the experimental precision, can be attributed to a lack of a complete characterization of the optical properties of the specific samples used in the experiment.

PACS numbers: 12.20.Fv,42.50.Lc

The Casimir force between two metallic layers arises from quantum mechanical fluctuations of the vacuum [1]. In recent years, an impressive amount of experimental [2, 3, 4] and theoretical [5, 6] work has been performed to better understand the Casimir force between real metals [7, 8, 9]. While most of the work has focused on cases where the attracting bodies are composed of the same material, the theoretical models also include the case of bodies composed of dissimilar metals [5].

Although the Casimir force is of fundamental importance in its own right, it is also an unwanted background in current attempts to search for new macroscopic forces over short distance scales [10]. Such forces have been conjectured to arise in unification theories, including those containing additional spatial dimensions [11]. It follows that setting stringent limits on new forces from Casimir force measurements requires either a very precise comparison between theory and experiment or a method for suppressing the Casimir background [12].

The preceding discussion provides the motivation for improving our understanding of the Casimir effect. More precise measurements should result in better theoretical models which, in turn, will yield a more complete picture of the Casimir effect, thus improving our ability to detect new macroscopic forces. Until recently, experiments lagged behind theory; with the development of sensitive force transducers, however, it became necessary to introduce refinements to the theory [5, 8].

In this Letter, we report the first precise measurement of the Casimir force between two dissimilar metals, at a precision  $\sim 100$  times better than previous measurements. At the current noise level of  $\sim 6 \text{ fN}/\sqrt{\text{Hz}}$  our data shows a small disagreement with the Lifshitz formula [13], which may be due to an incomplete characterization of the metallic dielectric function, as suggested in [8]. Our results thus suggest the need of additional experimental and theoretical work to further improve their agreement for the Casimir effect.

A microelectromechanical torsional oscillator (MTO) has been used since it is less affected by center of mass motions when compared with other systems. A judicious selection of the geometry results in a reduction of the spring constant  $\kappa$  of the system by over an order of magnitude. Furthermore, we used a dynamic scheme which fully exploits the high quality factor  $Q$  of the MTO.

The experimental setup is schematically shown in Fig. 1. An  $\text{Al}_2\text{O}_3$  sphere with a  $600 \mu\text{m}$  nominal diameter was sputter coated with a  $1 \text{ nm}$  layer of Cr followed by  $(203 \pm 6) \text{ nm}$  of

Au. After coating, the sphere was glued with conductive epoxy to the side of an Au coated optical fiber [3]. The radius of the coated sphere was measured to be  $(296 \pm 2) \mu\text{m}$ , the error arising because the  $\text{Al}_2\text{O}_3$  ball was not spherical. On the other hand, asymmetries induced by the deposition process were measured to be smaller than 10 nm, the resolution of the scanning electron microscope used. The fiber-sphere assembly was moved vertically by a micrometer driven stage in combination with a piezo-driven one.

The MTO is made of a  $3.5 \mu\text{m}$  thick,  $500 \times 500 \mu\text{m}^2$  heavily doped polysilicon plate suspended at two opposite points by serpentine springs, as shown in the inset of Fig. 2. The springs are anchored to a  $\text{SiN}_x$  covered Si platform. Two independent polysilicon electrodes under the plate allow the capacitance between the electrodes and the plate, which are separated by a gap of  $2 \mu\text{m}$ , to be measured. We calculated  $\kappa = (wt^3 E_{si}/6L_{serp}) \simeq 9.5 \times 10^{-10} \text{Nm/rad}$  [14], where  $w = 2 \mu\text{m}$  is the width of the serpentine,  $t = 2 \mu\text{m}$  its thickness and  $L_{serp} = 500 \mu\text{m}$  its length.  $E_{Si} = 180 \text{GPa}$  is Si Young's modulus. This value is in good agreement with the measured  $\kappa = 8.6 \times 10^{-10} \text{Nm/rad}$ . The MTO is mounted on a piezo electric driven  $xyz$  stage which in turn is mounted on a micrometer controlled  $xy$  stage. The edges of the plate are coated with 1 nm of Cr followed by 200 nm of Cu.

The combination of all translational stages allows positioning the Au coated sphere on top of the metal coated platform. The separation between the sphere and the platform is controlled by the  $z$ -axis of the  $xyz$  piezo stage. A two color fiber interferometer based closed-loop system is used to keep the fiber-to-platform separation  $z_i$  constant. The separation  $z_{metal}$  between the two metallic surfaces is (see Fig. 1):  $z_{metal} = z_i - z_o - z_g - b\theta$ , where  $b$  is the lever arm between the sphere and the axis of the MTO,  $\theta$  is the angle between the platform and the plate, and  $\theta \ll 1$  has been used.  $z_o$  was measured interferometrically by gently touching the platform with the sphere.  $z_g = (5.73 \pm 0.08) \mu\text{m}$ , which includes the gap between the platform and the plate, the thickness of the plate, and the thickness of the Cu layer, was determined using an AFM. The error in the interferometric measurements was found to be  $\Delta z_i^{rms} = 0.32 \text{nm}$ , which incorporates the relative vibrations of the fiber with respect to the platform and the measurement noise. The entire system was kept at a pressure below  $10^{-4}$  torr.

The force between the two metallic layers is determined by measuring the angle  $\theta$  as a function of the separation between the layers. Since  $\theta \ll 1$ , to a very good approximation  $\theta \propto \Delta C$ , where  $\Delta C$  is the difference in capacitance between the two electrodes and the

platform. The proportionality constant is found by applying a known potential difference between the two metallic layers at separations larger than  $3 \mu\text{m}$ . Thus, the net force can be approximated by the electrostatic force  $F_e$  [16]

$$F_e = 2\pi\epsilon_o(V_{Au} - V_o)^2 \sum_{n=1}^{\infty} \frac{[\coth(u) - n \coth(nu)]}{\sinh(nu)}, \quad (1)$$

where  $\epsilon_o$  is the permittivity of free space,  $V_{Au}$  is the voltage applied to the sphere,  $V_o$  the residual potential difference between the metallic layers when they are both grounded, and  $\cosh u = [1 + (z_{metal} + 2\delta_o)/R]$ . In Eq. (1) it was found that only the first two terms of the  $(z_{metal} + 2\delta_o)/R$  expansion give a significant contribution. The average separation between the layers when the metals come in contact,  $2\delta_o$ , is determined by the roughness of the films. As shown in Fig. 2, Eq. (1) can be used to fit the measured force between the plane and the sphere as a function of their separation for several values of  $V_{Au} - V_o$ , where  $V_o$  arises mainly from the difference between the work functions of the two metals. Eq. (1) serves several additional purposes: i) It is used to calibrate the constant between the measured  $\Delta C$  and the applied force. ii) It is used to find the voltage  $V_{Au}$  where the electrostatic force is zero, independent of the separation. iii) It is also used to fit for the radius of the Au coated sphere  $R = (294.3 \pm 0.1) \mu\text{m}$ , and iv) for the increase in the separation between the two metallic layers,  $2\delta_o$ . The fitted value of  $\delta_o = (39.4 \pm 0.3) \text{ nm}$  agrees with the value estimated from AFM measurements,  $\delta_o = (33 \pm 9) \text{ nm}$ . Furthermore, it was found that the motion of the sphere parallel to the axis of the MTO did not affect  $\theta$ , while its motion perpendicular to the axis resulted in a linear dependence on  $b$ . We thus conclude that there are no significant deviations from the assumption that the Cu plane is of infinite extent.

The force between the two metals is  $F = k\Delta C$ , where  $\Delta C$  is measured to 1 part in  $5 \times 10^5$  using a bridge circuit [17]. The constant  $k$  is determined by Eq. (1) to be  $k = (50280 \pm 6) \text{ N/F}$ . With this approach the force sensitivity was found to be  $1.4 \text{ pN}/\sqrt{\text{Hz}}$ . By setting  $V_{Au} = V_o = 0.6325 \text{ V}$ , the Casimir force between the Au coated sphere and the Cu planar film was determined. The measurements are shown in Fig. 3(a).

To improve on the force sensitivity, a direct use of the high quality factor of the MTO was implemented [4]. In this approach the vertical separation between the sphere and the oscillator was changed as  $\Delta z_{metal} = A \cos(\omega_r t)$ , where  $\omega_r$  is the resonant angular frequency of the MTO, and  $A$  was adjusted between 3 and 35 nm for  $z_{metal}$  equal to 0.2 and 1.2  $\mu\text{m}$ ,

respectively. The solution for the oscillatory motion yields [4]

$$\omega_r = \omega_o \left[ 1 - \frac{b^2}{2I\omega_o^2} \frac{\partial F_c}{\partial z} \right], \quad (2)$$

where  $\omega_o \simeq \sqrt{\kappa/I}$  for  $Q \gg 1$ , and  $I \simeq 4.6 \times 10^{-17}$  kg m<sup>2</sup> is the moment of inertia. Since  $A \ll z_{metal}$ , terms of higher order in  $\theta$  introduce a  $\sim 0.1\%$  error. As before, Eq. (1) was used to calibrate all constants. We found  $\omega_o = 2\pi$  (687.23 Hz), and  $b^2/2I = 6.489 \times 10^8$  kg<sup>-1</sup>. With an integration time of 10 s using a phase lock loop circuit [15], changes in the resonant frequency of 10 mHz were detectable. This allows the force to be calculated with a sensitivity of the order of  $\delta F_c = 6$  fN/ $\sqrt{\text{Hz}}$ , a factor  $\sim 3$  larger than the thermodynamic noise. The results for these measurements are plotted in Fig. 4.

In this configuration  $\partial F_c/\partial z$  is being measured. Using the proximity force theorem [18], the Casimir force  $F_c$  between a spherical surface of radius  $R$  and an infinite plane is given by  $F_c = -\pi^3 \hbar c R / 360 z^3$  [19], where  $c$  is the speed of light in vacuum and  $\hbar$  is Planck's constant. Its derivative  $\partial F_c/\partial z = 2\pi R P_c$ , where  $P_c$  is the force per unit area between two infinite planes.

When finite conductivity effects are taken into account, the Casimir force per unit area between two planes  $P_{CP}$ , and the force between a sphere and a plane  $F_{CS}$ , are given by [5, 13]

$$P_{CP} = -\frac{\hbar}{2\pi^2 c^3} \int_0^\infty \xi^3 d\xi \int_1^\infty p^2 \left\{ \left[ \frac{(s_1+p)(s_2+p)}{(s_1-p)(s_2-p)} e^{2p\xi z/c} - 1 \right]^{-1} + \left[ \frac{(s_1+\epsilon_1 p)(s_2+\epsilon_2 p)}{(s_1-\epsilon_1 p)(s_2-\epsilon_2 p)} e^{2p\xi z/c} - 1 \right]^{-1} \right\} dp, \quad (3a)$$

$$F_{CS} = \frac{\hbar}{2\pi c^2} R \int_0^\infty \xi^2 d\xi \int_1^\infty p \left\{ \ln \left[ 1 - \frac{(s_1-p)(s_2-p)}{(s_1+p)(s_2+p)} e^{-2p\xi z/c} \right] + \ln \left[ 1 - \frac{(s_1-\epsilon_1 p)(s_2-\epsilon_2 p)}{(s_1+\epsilon_1 p)(s_2+\epsilon_2 p)} e^{-2p\xi z/c} \right] \right\} dp, \quad (3b)$$

where  $\epsilon_j(i\xi)$  is the dielectric function of metal  $j$ ,  $\omega = i\xi$  is the complex frequency, and  $s_j = \sqrt{\epsilon_j - 1 + p^2}$ . Since the metals are not smooth, the expressions in Eq. (3) should be averaged over different possible separation distances determined by the surface roughness [20],

$$P_C = \sum_i w_i P_{CP}(z_i), \quad (4a)$$

$$F_C = \sum_i w_i F_{CS}(z_i), \quad (4b)$$

to model the data shown in Figs. 3 and 4. The probabilities  $w_i$  were found using the AFM profiles of the interacting surfaces. The values of the dielectric constant for Au and Cu were obtained from [21], extended to low energies using a Drude model [9]. The agreement between model and data is better than 1% for all cases where  $\delta F(z) \leq 0.01F(z)$ , *i.e.*  $z < 0.5 \mu\text{m}$ .

There are, however, measurable differences between the experimental and theoretical values of the Casimir energy. Although the differences are larger than the experimental error, they likely arise from the  $\epsilon(\omega)$  used, not necessarily reflecting shortcomings of Eq. (3): Using different optical constants for Au and Cu [22], or different models of roughness, results obtained from Eq. (4) vary by more than 1%.

Other possible sources of discrepancy are: i) finite thickness of the metallic layers, and ii) effects of temperature. Since the layers are much thicker than the penetration depth of electromagnetic radiation on the system [5], we can treat them as effectively infinite. Finite temperature corrections have been found to be  $\lesssim 0.1\%$  using a plasma dispersion model [5]. Other approaches [23] predict corrections of up to 15%. Although these corrections have the same sign as the deviation observed in our experiment, our data do not support their results. The sensitivity is such that the effect of thermal corrections should be taken into account once the metals are fully characterized.

Given the improved sensitivity of our measurement of the Casimir force, we can set more stringent limits on new macroscopic forces acting over short separations. A new force would appear as a perturbation to the usual gravitational potential energy [24]. Such perturbation, a Yukawa interaction, is characterized by its strength  $\alpha$  and its range  $\lambda$ . Using the differences of Fig. 3b as a benchmark for the manifestation of new forces, we can set a limit  $\alpha(\lambda = 200 \text{ nm}) \sim 10^{13}$ , which represents an improvement of a factor of 4 with respect to previously reported limits [12]. If, once the metals are properly characterized, the difference between the measured and calculated values of the Casimir force is found to be on the order of the experimental error, then at the  $1 \sigma$  level our results give  $\alpha(200 \text{ nm}) \leq 10^{11}$ . These limits can be improved by directly comparing the force between the sphere and two different metals, or two different isotopes of the same element [25]. Such measurements are presently underway, and will be presented elsewhere.

In summary, it was shown that by using a MTO, the sensitivity in the force between two metallic films is improved by  $\sim 100$  over previous experiments. This highlights the necessity

of a simultaneous measurement of the dielectric constant of the metallic films used in the force measurements, and a better understanding of the Casimir force between non-ideal bodies. When used to set new limits in the search for new forces, it is concluded that an improvement of more than 2 orders of magnitude can be achieved for separations  $\sim 100$  nm. The dynamic method employed also allows for a direct experimental test of the proximity force theorem.

We are deeply indebted to G. L. Klimchitskaya and V. M. Mostepanenko for help with the theoretical analysis. We also wish to thank H. B. Chan, A. Lambrecht, S. Reynaud, and U. Mohideen for useful discussions. RSD acknowledges financial support from the Petroleum Research Foundation through ACS-PRF#37542-G. The work of EF is supported in part by the U.S. Department of Energy under Contract No. DE-AC02-76ER071428.

- 
- [1] H. B. G. Casimir, Proc. K. Ned. Akad. Wet. **51**, 793 (1948). See Bordag, Mohideen, and Mostepanenko, Phys. Rep. **353**, 1 (2001) and Milton, *The Casimir Effect* (World Scientific, River Edge, NJ, 2001) for recent reviews.
  - [2] U. Mohideen and A. Roy, Phys. Rev. Lett. **81**, 4549 (1998); A. Roy and U. Mohideen, Phys. Rev. Lett. **82**, 4380 (1999); S. K. Lamoreaux, Phys. Rev. Lett. **78**, 5 (1997); B. W. Harris, F. Chen, and U. Mohideen, Phys. Rev. A**62**, 052109 (2000); G. Bressi *et al.*, Phys. Rev. Lett. **88**, 041804 (2002); F. Chen *et al.*, Phys. Rev. Lett **88**, 101801 (2002).
  - [3] H. B. Chan *et al.*, Science **291**, 1941 (2001).
  - [4] H. B. Chan *et al.*, Phys. Rev. Lett. **87**, 211801 (2001).
  - [5] B. Geyer, G. L. Klimchitskaya, and V. M. Mostepanenko, Phys. Rev. A**65**, 062109 (2002).
  - [6] F. Chen *et al.*, Phys. Rev. A**66**, 032113 (2002).
  - [7] G. L. Klimchitskaya, U. Mohideen, and V. M. Mostepanenko, Phys. Rev. A**61**, 062107 (2000).
  - [8] S. K. Lamoreaux, Phys. Rev. A**59**, R3149 (1999).
  - [9] A. Lambrecht and S. Reynaud, Eur. Phys. J. D **8**, 309 (2000); C. Genet, A. Lambrecht, and S. Reynaud, Phys. Rev A **62**, 012110 (2000).
  - [10] D. E. Krause and E. Fischbach, *Gyros, Clocks, and Interferometers: Testing Relativistic Gravity in Space*, edited by C. Lämmerzahl, C. W. F. Everitt, and F. W. Hehl (Springer-Verlag, NY, 2001).

- [11] L. Randall, *Science* **296**, 1422 (2002).
- [12] E. Fischbach *et al.*, *Phys. Rev. D* **64**, 075010 (2001); D. E. Krause and E. Fischbach, *Phys. Rev. Lett.* **89**, 190406 (2002); D. E. Krause *et al.*, *The Ninth Marcel Grossmann Meeting*, edited by V. G. Gurzadyan, R. T. Jantzen, and R. Ruffini (World Scientific, Singapore, 2002).
- [13] E. M. Lifshitz, *Zh. Eksp. Teor. Fiz.* **29**, 94 (1956)[*Sov. Phys. JETP* **2**, 73 (1956)]
- [14] S. D. Senturia, *Microsystem Design* (Kluwer Academic Publishers, Boston, 2001).
- [15] R. S. Decca, H. D. Drew, and K. L. Empson, *Rev. Sci. Instrum.* **68**, 1291 (1997).
- [16] W. R. Smythe, *Static and Dynamic Electricity* (McGraw-Hill, New York, 1939).
- [17] P. W. Kolb, R. S. Decca, and H. D. Drew, *Rev. Sci. Instrum.* **69**, 310 (1998).
- [18] J. Blocki *et al.*, *Ann. Phys. (N.Y.)* **105**, 427 (1977).
- [19] B. V. Derjaguin, I. I. Abrikosova, and E. M. Lifshitz, *Q. Rev. Chem. Soc.* **10**, 295 (1956).
- [20] G. L. Klimtchiskaya *et al.*, *Phys. Rev. A* **60**, 3487 (1999).
- [21] *Handbook of Optical Constants of Solids*, edited by E. D. Palik (Academic, New York, 1985).
- [22] P. B. Johnson and R. W. Christy, *Phys. Rev. B* **6**, 4370 (1972).
- [23] M. Boström and B. E. Sernelius, *Phys. Rev. Lett.* **84**, 4757 (2000); B. Høye *et al.*, quant-ph/0212125 [to appear in *Phys. Rev. E*].
- [24] E. Fischbach and C. L. Talmadge, *The Search for Non-Newtonian Gravity* (AIP/Springer-Verlag, NY, 1999).
- [25] R. S. Decca, D. López, H. B. Chan, E. Fischbach, and D. E. Krause (unpublished).



## Figures

FIG. 1: Schematic of the experimental setup showing its main components. The inset shows an schematic of the electronic circuit used for the static measurements.

FIG. 2: Electrostatic force as a function of separation for  $V_{Au} - V_o = 0.24$  V and 0.30 V. Inset: Scanning electron microscope image of the MTO showing the serpentine spring.

FIG. 3: Casimir force as a function of separation. The separation between the metallic layers has been adjusted to account for the roughness:  $z = z_{metal} + 2\delta_o$  **(a)** Direct measurement of the force. The solid line is a fit using Eq. (4b). **(b)** Experimental data subtracted from the theoretical model.

FIG. 4: **(a)** Derivative of the Casimir force (see text) as a function of separation. The solid line is a fit using Eq. (4a). **(b)** Experimental data subtracted from the theoretical model. The deviation with respect to the model at small separations is partially associated with non-linear terms on Eq. (2).

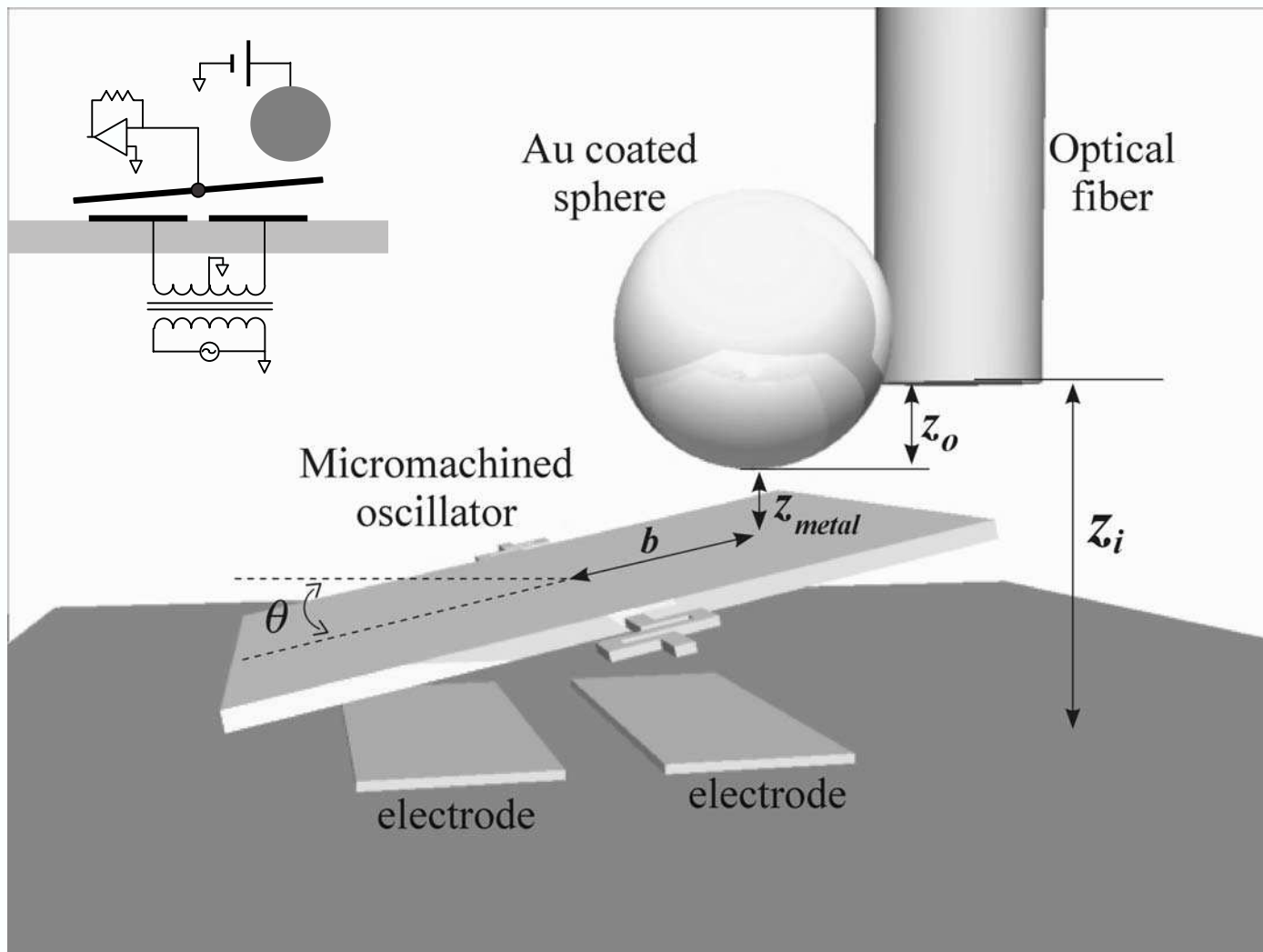


Fig. 1: Decca et al.

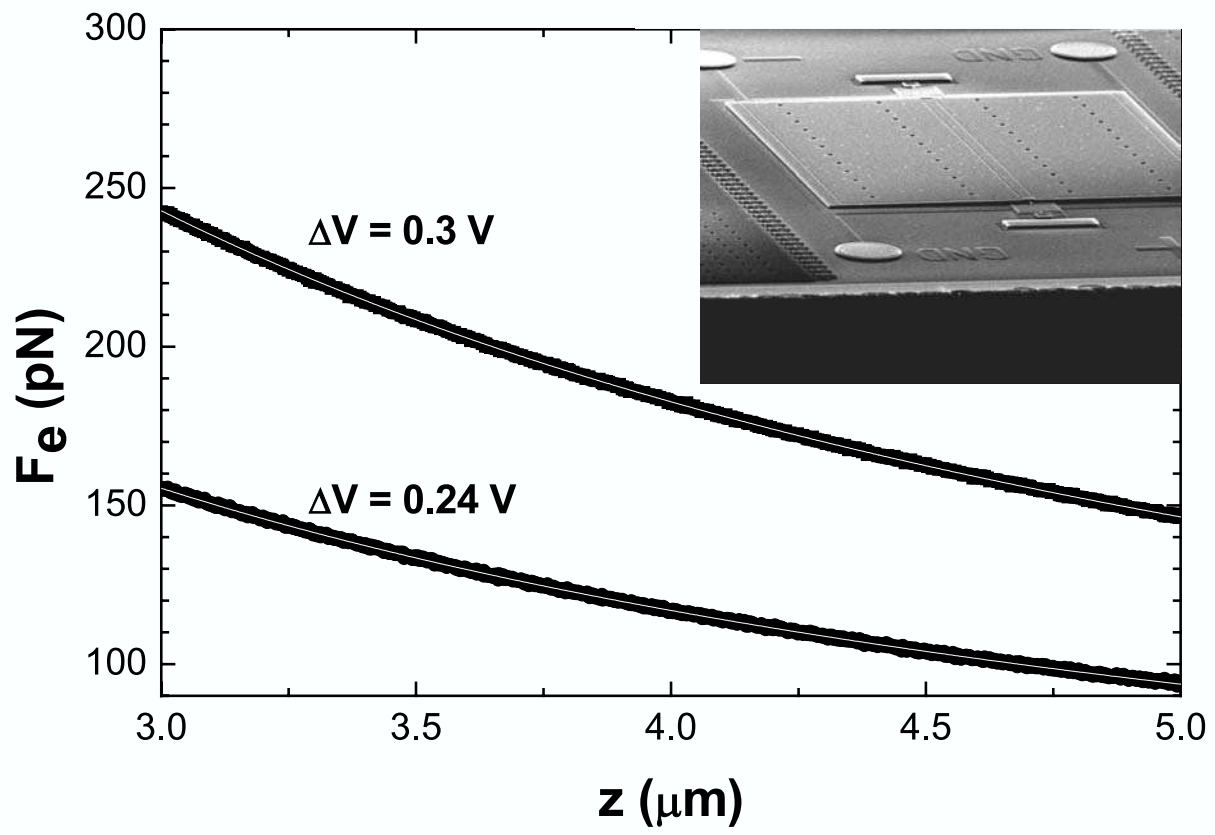


Fig. 2: Decca et al.

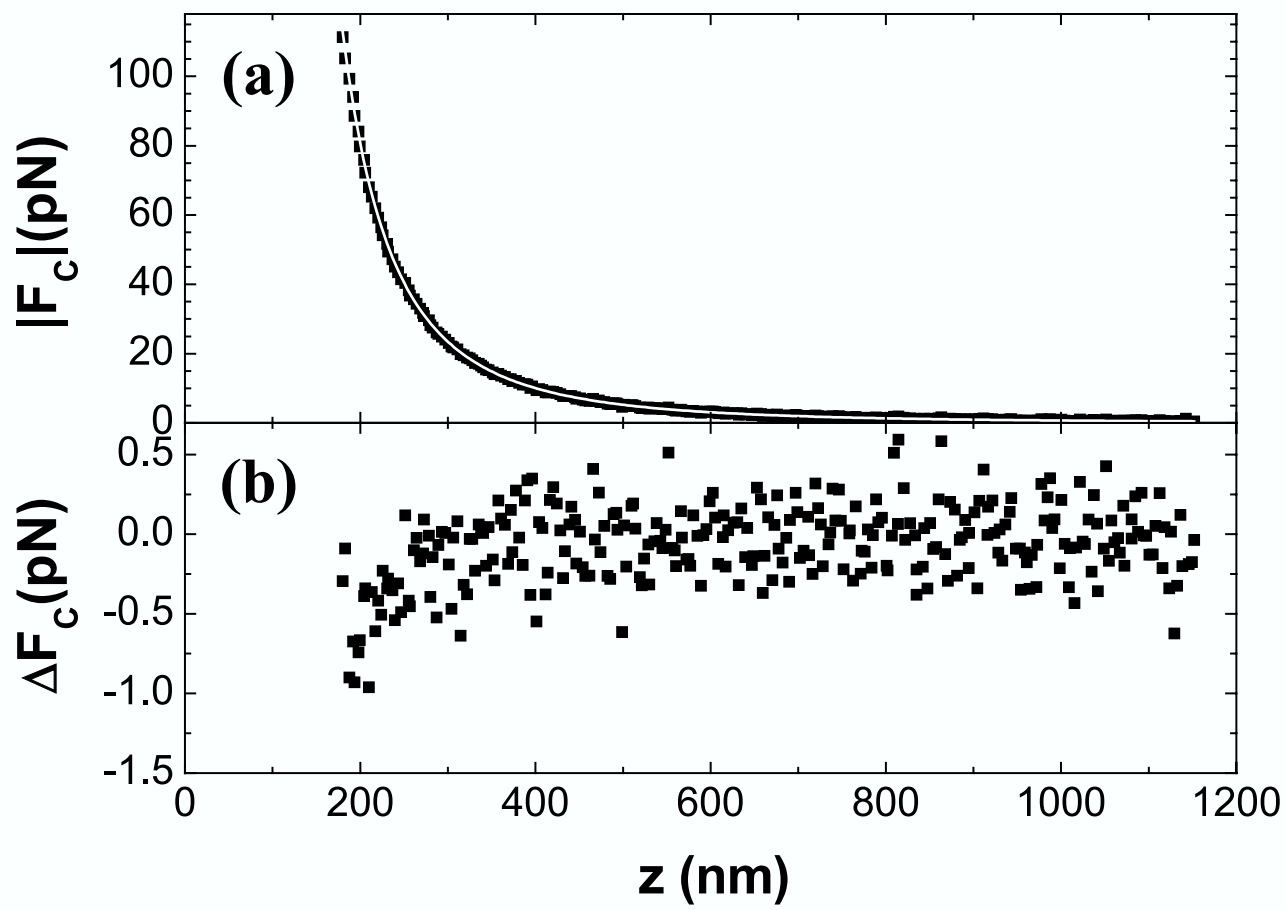


Fig. 3: Decca et al.



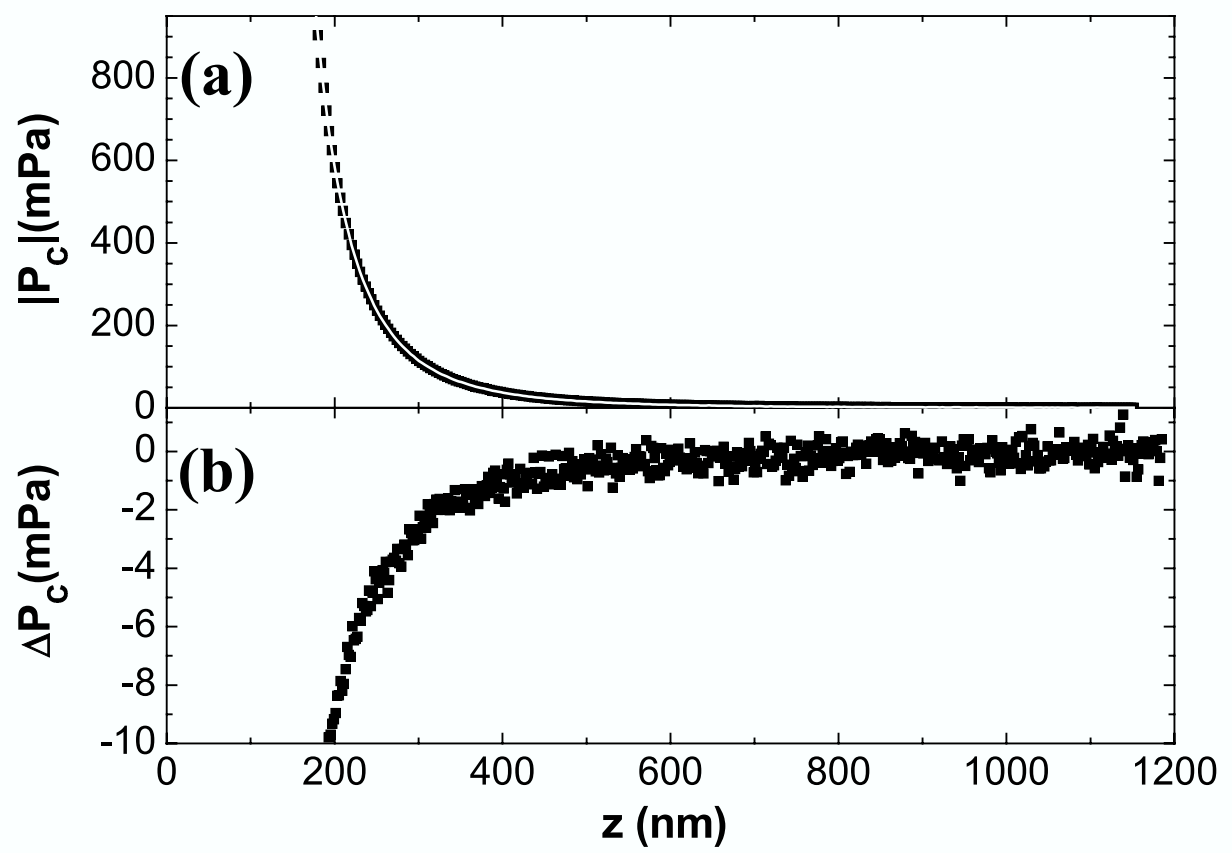


Fig. 4: Decca et al.